Mutual influence of molecular diffusion in gas and surface phases

Takuma Hori,* Takafumi Kamino, Yuta Yoshimoto, Shu Takagi, and Ikuya Kinefuchi†
Department of Mechanical Engineering, The University of Tokyo, 7-3-1 Hongo, Bunkyo-ku, Tokyo 113-8656, Japan

(Received 9 August 2017; published 3 January 2018)

We develop molecular transport simulation methods that simultaneously deal with gas- and surface-phase diffusions to determine the effect of surface diffusion on the overall diffusion coefficients. The phenomenon of surface diffusion is incorporated into the test particle method and the mean square displacement method, which are typically employed only for gas-phase transport. It is found that for a simple cylindrical pore, the diffusion coefficients in the presence of surface diffusion calculated by these two methods show good agreement. We also confirm that both methods reproduce the analytical solution. Then, the diffusion coefficients for ink-bottle-shaped pores are calculated using the developed method. Our results show that surface diffusion assists molecular transport in the gas phase. Moreover, the surface tortuosity factor, which is known to be uniquely determined by physical structure, is influenced by the presence of gas-phase diffusion. This mutual influence of gas-phase diffusion and surface diffusion indicates that their simultaneous calculation is necessary for an accurate evaluation of the diffusion coefficients.

DOI: 10.1103/PhysRevE.97.013101

I. INTRODUCTION

Understanding molecular diffusion phenomena in porous media is of great importance for improving the performance of various applications, such as membrane gas separation [1–3], fuel cell power generation [4,5], and shale gas purification [6,7]. Since most of these porous media have nanoscale pores, the predominant flow regime in them is Knudsen diffusion. Such systems cannot be treated as a continuum flow since molecular scale phenomena become dominant. Numerical simulation is a promising approach for probing molecular behavior even in complex structures. While the most widely used method to track molecular trajectories is molecular dynamics simulation, which solves Newton's equations of motion to obtain the time evolution of the positions and velocities, its computational cost is too high for it to be applied to porous media. Thus one simulation method commonly used for porous media is the direct simulation Monte Carlo (DSMC) method [8], a stochastic way to solve the Boltzmann transport equation in Knudsen flow. The computational cost of DSMC is low compared with molecular dynamics since intermolecular and molecule-surface collisions are treated by collision models rather than by rigorously solving the equations of motion of all the atoms in the system. The DSMC method can distinguish molecular species and simulate molecular diffusion phenomena incorporating intermolecular collisions. Meanwhile, the test particle method [9] and the mean square displacement (MSD) method [10] are known to be simpler simulation methods for solving steady state diffusion phenomena than the DSMC method. In the test particle and MSD methods, molecular species are not addressed explicitly; rather, the molecular velocity and mean free path are imposed as constant values. Owing to their simplicity and generality, many numerical studies on molecular transport in porous media utilize these methods [11–15].

In addition to Knudsen diffusion, surface diffusion [16,17] can affect molecular transport when the pore size is sufficiently small. Here, surface diffusion is a form of diffusion in which molecules diffuse on the pore surfaces after being adsorbed on them. Previous experiments show that surface diffusion contributes significantly to the overall diffusion in meso- and micropores [18–22]. As for theoretical analyses of surface diffusion, previous studies have focused on systems involving a simple cylinder or two-dimensional systems [23–26]. Meanwhile, numerical simulations are applicable to analyses of not only the gas phase but also surface-phase diffusion in complex structures. In fact, many numerical simulations of surface diffusion have been reported [27–29]. For instance, the relationship between tortuosity factors for gas and surface phases was discussed by using the MSD method for surfaces of complex porous structures [29]. These successful studies focused on diffusion phenomena occurring only on the surface, and did not simultaneously analyze those in the gas phase. However, actual molecules experience repeated adsorption (desorption) on (from) surfaces; thus gas- and surface-phase diffusions occur at the same time. The impact of simultaneous gas- and surface-phase diffusions on the overall diffusion coefficient has remained unclear. This effect must be elucidated for a better and more quantitative understanding of the diffusion of molecules in porous structures.

We develop a method to simulate molecular transport incorporating surface diffusion in addition to gas-phase diffusion. The validity of the simulations is confirmed using a simple cylindrical structure, by comparing calculated results with theoretical solutions. By utilizing the developed method, we examine how the surface diffusion phenomena affect the overall diffusion coefficient in ink-bottle structures, which, unlike a simple cylinder, exhibit surface tortuosity.

*hori@fel.t.u-tokyo.ac.jp
†kine@fel.t.u-tokyo.ac.jp

II. SIMULATION METHODS

A. Evaluation of the diffusion coefficient

We develop two simulation methods to determine the effect of surface diffusion on the overall diffusion coefficient. Both methods are based on traditional simulation techniques: one, on the test particle method [9]; the other, on the MSD method [10]. The former technique calculates the molecular diffusivity under a steady state. Since the results obtained by this method have a significant dependence on the system size, a sufficiently large computational domain in the flow direction is necessary. Meanwhile, the MSD method involves a simulation based on Brownian motion. This method does not yield accurate diffusion coefficients in porous media with dead-end pores. It has been reported that these two methods give almost the same diffusion coefficient in porous media without dead-end pores [11]. A convective flow is not treated in these methods, unlike in the DSMC [30]. We first present the details of the two methods and then explain how to incorporate the surface diffusion phenomenon into them.

In the test particle method, the transmission probability f of molecules from one side of an entire structure to the opposite side at a distance L_t is calculated. Once the transmission probability f is obtained, the diffusion coefficient is calculated via

$$D_{TP} = \frac{1}{4} f L_t v, \tag{1}$$

where v is the molecular velocity. As the initial state, a molecule is introduced on one side of the simulation domain (i.e., incident surface). The initial position is selected randomly on the incident surface. The initial direction is determined by the Knudsen cosine law [31]. After the initial conditions are assigned, the molecule moves repeatedly with time steps of Δt. During its motion, the molecule may experience collisions with background gas molecules, which are implicitly considered in the simulation; the direction of the molecule is changed randomly to imitate intermolecular collisions approximately. The collision occurs with a probability $P = 1 - \exp[-v\Delta t/\Lambda]$, where Λ is the mean free path. The molecule also experiences collisions with solid surfaces. After a collision with a solid surface, the direction of the scattered molecule is reassigned according to reflection models based on specular or diffuse reflection. The molecular motion and these collision events are calculated iteratively until the molecule returns to the incident surface or reaches the opposite surface. Many particles are introduced repeatedly to obtain the transmission probability.

The MSD method is based on the random walk of a Brownian particle; the theoretical background of the MSD method can be found in a previous work [32]. The diffusion coefficient can be obtained in terms of the porosity ε of the structure via

$$D_{MSD} = \lim_{t\to\infty} \varepsilon \frac{\langle \xi_x^2 \rangle}{2t}, \tag{2}$$

where t is the travel time and $\langle \xi_x^2 \rangle$ is the MSD of molecules in the x direction. In the MSD method, the initial coordinate of a molecule is chosen randomly in the voids of the structure. The motion and collisions of the molecule are simulated in the same way as in the test particle method, where the displacement ξ_x is sampled at each time step. The molecular movement and collision are iterated until the total simulation time reaches a prescribed time t_{MSD}. The MSD is calculated by repeating the above process, and then the diffusion coefficient is obtained from Eq. (2). In practice, diffusion coefficients are determined by omitting the initial rising part of the MSD and fitting the remaining part to a linear function with respect to time.

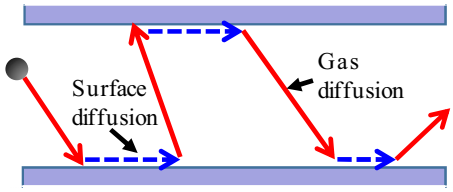

FIG. 1. Schematic of concurrent gas and surface diffusion in a cylindrical pore. Rather than undergoing desorption immediately after molecule-surface collision, molecules move along the surface over a certain distance according to a given surface diffusion coefficient and time.

B. Incorporation of surface diffusion into simulations

Surface diffusion is incorporated into the above two simulations, as illustrated in Fig. 1: Molecules diffuse on solid surfaces after colliding with them, instead of being reflected immediately as is often the case in conventional simulations. Assuming that the direction of diffusion on solid surfaces is isotropic, the diffusion distance r can be determined from the probability distribution $C(r)$, which is the solution of the two-dimensional diffusion equation:

$$C(r) = \frac{r}{2D_s t_{as}} \exp\left(\frac{r^2}{4D_s t_{as}}\right), \tag{3}$$

where D_s is the surface diffusion coefficient and t_{as} is the surface residence time. Equation (3) does not take into account the blocking effect of molecules adsorbed on the surface [33]. t_{as} is determined by the probability distribution $\exp(-t/t_s)/t_s$, where t_s is the average surface diffusion time. Thus the surface diffusion distance is governed by the product of the two parameters D_s and t_s. The parameters are widely changed to quantify the effect of surface diffusion on the overall diffusion coefficient, as demonstrated in the next section.

As discussed above, the effect of surface diffusion is incorporated by moving the molecules on the surface by a distance r after collision, associated with the behavior of molecules on surfaces without forming any chemical bonds [34,35]. The direction of surface diffusion is set to be isotropic unless stated otherwise. Here, in the test particle method, the surface diffusion time t_{as} does not influence the results because Eq. (1) does not explicitly depend on time. In the MSD method, however, the diffusion time on the surface affects the results since the time evolution of the displacement is tracked. The introduction of surface diffusion results in uneven time intervals for sampling molecular displacements, unlike in the standard MSD method, since gas-phase diffusion is tracked at constant intervals of Δt while the surface diffusion time varies with the probability $\exp(-t/t_s)/t_s$, which is typically different from Δt. Thus we divide the elapsed time into uniform bins of Δt to determine the MSD.

In the following section, the test particle and MSD methods are performed for simple cylindrical and ink-bottle pores. We set Δt equal to $5.0 \times 10^{-3}\, L/v$, where L is the characteristic pore length. For the reflection model, diffuse reflection is adopted, where a molecular speed remains constant before and after the collision with surfaces. We have dealt only with the diffuse reflection model to extensively evaluate the surface diffusion effect and to facilitate a comparison of numerical results with analytical solutions. Unless noted otherwise, the mean free path is set to infinity, which corresponds to Knudsen diffusion. 1 000 000 and 1000 molecules are simulated for the test particle and MSD methods, respectively, with $t_{\mathrm{MSD}} = 2.0 \times 10^{7}\, \Delta t$. We note that all surfaces are constructed by triangular elements. During surface diffusion, when a molecule on the surface reaches the edge of a triangular element, it moves to the neighboring triangular element. At the same time, the direction of the molecule is changed since the normal vectors of the two triangles are different. The new direction is determined by rotating the old direction by the angle between the two normal vectors.

III. RESULTS AND DISCUSSION

A. Surface diffusion effect in a cylindrical pore

To validate our simulation method, molecular transport simulations are performed in a simple cylindrical pore. The cylindrical pore structure is approximated by a polygonal column with a regular 36-sided polygonal cross section. We define the diameter of the cylindrical pore L_{d} as the characteristic length. The analytical solution of the diffusion coefficient in the presence of surface diffusion in a cylindrical pore, which holds for any Knudsen number, is given by [23,26]

$$D = D_{\mathrm{g}} + \frac{D_{\mathrm{s}} t_{\mathrm{s}}}{t_{\mathrm{g}}}. \tag{4}$$

Here, D_{g} is the diffusion coefficient in the gas phase, and t_{g} is the average flight time between pore walls. As in the case of Eq. (3), Eq. (4) assumes that the direction of surface diffusion is isotropic. It is widely known that D_{g} and t_{g} are equal to $L_{\mathrm{d}} v/3$ and L_{d}/v, respectively, in a cylindrical pore when the Knudsen number ($\mathrm{Kn} = \Lambda/L_{\mathrm{d}}$) is infinity [36]. We note that Eq. (4) is based on the assumption that the adsorbed molecules never affect the molecular diffusion in a gas phase, thus resulting in an increase of diffusion paths for molecules represented by the second term of the right-hand side.

Simulations of the test particle method are performed with various $D_{\mathrm{s}} t_{\mathrm{s}}$ and Kn values. It is known that the method underestimates the diffusion coefficient when the pore length is short [37]. Therefore, the cylinder length is set to $500 L_{\mathrm{d}}$, which is long enough to obtain an accurate value. The calculated results are compared with the analytical solution in Fig. 2. We note that the D_{g} and t_{g} values substituted into Eq. (4) are not known when Kn is finite. Thus D_{g} is calculated by the test particle method without considering the surface diffusion effect and then substituted into Eq. (4). The t_{g} values are sampled during the simulations, and it is found that under any condition they are equal to L_{d}/v, which is the analytical solution of t_{g} in the case of $\mathrm{Kn} = \infty$. As can be seen from Fig. 2, the diffusion coefficients obtained by the test particle simulation agree well with Eq. (4) when Kn is infinity, which

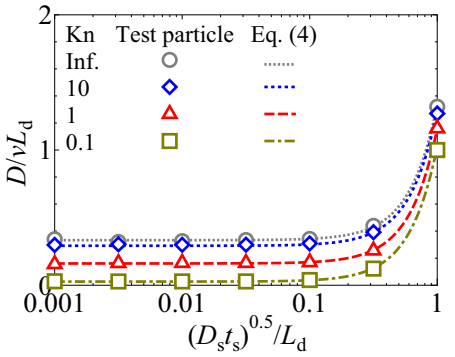

FIG. 2. Dependence of diffusion coefficient on $(D_{\mathrm{s}}t_{\mathrm{s}})^{0.5}/L_{\mathrm{d}}$ in a cylindrical pore, as calculated by the test particle method. The calculated results are compared with the analytical solutions given by Eq. (4).

indicates the validity of our simulation. As for the other Kn conditions, the calculated diffusion coefficients agree well with the analytical solutions in those cases, too. Thus the analytical solution given by Eq. (4) can accurately yield the diffusion coefficient for any Kn.

In the theoretical solutions and simulations described above, the surface diffusion direction of a molecule is chosen randomly, regardless of the incident direction. However, the diffusion direction on the surfaces might be influenced by the incident direction [34], since it is unrealistic to assume that an incident molecule would lose all its momentum immediately after collision with the surface. Our simulation method can easily incorporate such anisotropy in surface diffusion, while it would be difficult for theoretical models. Thus we quantify the influence of surface diffusion anisotropy on the overall diffusion coefficient. In the extreme case, the direction of surface diffusion is determined completely by that of the incident molecule. More specifically, the new direction is assigned by projecting the direction of the incident molecule on the surface. The surface diffusion distance is subject to the distribution given by Eq. (3). The calculated results are shown in Fig. 3. It can be seen that the diffusion coefficient becomes larger by setting an anisotropic direction for surface diffusion. Therefore, when surface diffusion has a significant influence on molecular transport, the surface diffusion direction should

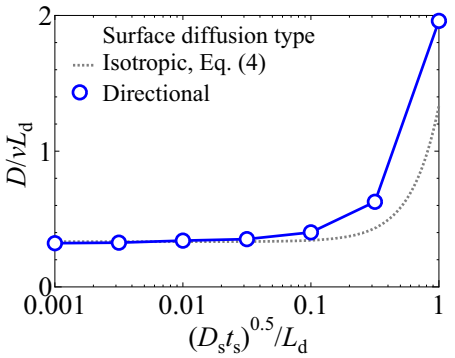

FIG. 3. Comparison of diffusion coefficients for a cylindrical pore with isotropic or directional surface diffusion. The Knudsen number is set to infinity. The isotropic curve is calculated from Eq. (4), while the directional diffusion data are calculated by the test particle method.

be considered to obtain an accurate value for the diffusion coefficient. As demonstrated, it is possible to quantify the influence of surface diffusion directionality on the diffusion coefficients, which is not achievable by the theoretical approach.

B. Comparison of the test particle and MSD methods

In the test particle method, the calculated diffusion coefficients do not explicitly depend on time, as shown in Eq. (1). The individual contributions of D_s and t_s to the overall molecular transport are indistinguishable, while their product affects the surface diffusion, as shown in Eq. (3). Meanwhile, the diffusion coefficient obtained from the MSD method is clearly influenced by time, as indicated by Eq. (2). Thus D_s and t_s are independent parameters, unlike in the test particle method. This difference can be attributed to the difference in the definitions of diffusion coefficients. Molecular flux q can be expressed in terms of the diffusion coefficient and the molecular concentration distribution as

$$q = -D\frac{dC_g}{dx}, \tag{5}$$

where C_g is the concentration distribution of molecules in the gas phase. Since the concentrations at both ends of the computational domain are implicitly imposed in the test particle method, the diffusion coefficient obtained by this method, D_{TP}, corresponds to the diffusivity, D, in Eq. (5). Meanwhile, concentration can be defined in another way in the presence of surface diffusion: It is possible to count not only the gas-phase molecules but also those on the surface in the concentration. The concentration distribution of molecules in both the gas and surface phases, C_t, is related to C_g via the equation [26]

$$\frac{C_t}{C_g} = \frac{t_g + t_s}{t_g}. \tag{6}$$

Here, the above ratio is assumed to be constant at any x coordinate. Then, q can be reformulated as

$$q = -D_t\frac{dC_t}{dx}. \tag{7}$$

The two diffusion coefficients defined in different ways can be organized via Eq. (6). D_t in Eq. (7) is derived by utilizing the density gradient of molecules in both the gas and surface phases, thus representing the diffusion coefficient per molecule. Therefore, D_t must be equal to the diffusion coefficient obtained by the MSD method, D_{MSD}, which tracks the diffusion of a single molecule.

The relationship between these diffusion coefficients, D and D_t, in Eqs. (5) and (7), is confirmed by comparing the results of the two methods. The parameter $D_s t_s$ is fixed by $(D_s t_s)^{0.5}/L_d = 1$, with various $t_s/(L_d/v)$ values ranging from 0.001 to 10. Figure 4 compares the results. While the diffusion coefficients obtained by the test particle calculations are constant, those obtained by the MSD method strongly depend on $t_s/(L_d/v)$, as expected. The diffusion coefficients of the MSD method are divided by $(t_g + t_s)/t_g$, as expressed in Eq. (6), to elucidate the relationship between these two methods. Here, t_s/t_g is sampled during the MSD simulations. Figure 4 compares D_{TP}, D_{MSD}, and $D_{MSD}[(t_g + t_s)/t_g]^{-1}$. It is seen that the discrepancy between the two methods can be well explained by Eq. (6). We also confirm that the diffusion coefficient from the MSD method converges with that from the test particle method when $t_s/(L_d/v)$ is sufficiently small.

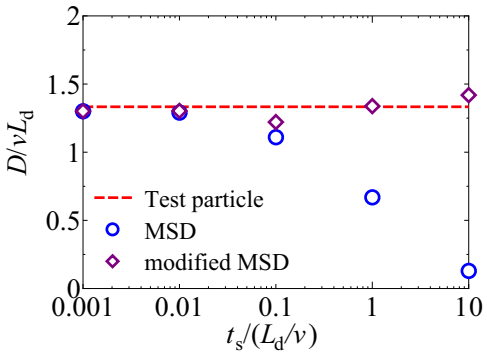

FIG. 4. Diffusion coefficients calculated by the test particle and MSD methods for $(D_s t_s)^{0.5}/L_d = 1$. The modified MSD results are obtained on the basis of Eq. (6), i.e., $D_{MSD}[(t_g + t_s)/t_g]^{-1}$.

We investigate the individual diffusivities of the gas and surface phases by the MSD method. The time evolutions of the displacements contributed by gas- and surface-phase diffusions can be sampled separately from the MSD simulations. More specifically, $\langle \xi_g^2 \rangle$ and $\langle \xi_s^2 \rangle$—where ξ_g and ξ_s are the cumulative displacement in the gas and surface phases, respectively—are evaluated. Figure 5 shows the separated MSDs calculated from the time evolutions of those displacements. The time in Fig. 5 is the gross diffusion time in the gas and surface phases. Here, the surface diffusion parameters are set to $D_s/(vL_d) = 1000$ and $t_s/(L_d/v) = 0.001$. The separated MSDs are clearly linear functions in the long-time region; thus their diffusion coefficients can be easily evaluated from the gradients. We have found that the calculated diffusion coefficient for the gas phase is $D_g/(vL_d) = 0.338$, which is in good agreement with the analytical solution, $D_g/(vL_d) = 1/3$. On the other hand, the diffusion coefficient for the surface phase must be evaluated from the MSD associated with the surface diffusion time, instead of the gross diffusion time. Thus the diffusion coefficient for the surface phase, obtained directly from Eq. (2), is divided by the diffusion time ratio $t_s/t_g = 0.001$. The diffusion coefficient obtained is $D_s/(vL_d) = 1001$, which reproduces well the inputted value of $D_s/(vL_d) = 1000$. These results indicate that the separation of the MSD can successfully yield the contributions from each phase.

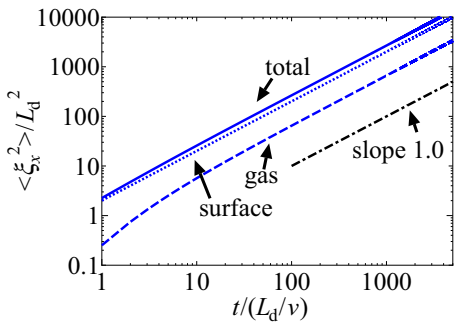

FIG. 5. MSDs under the conditions $D_s/(vL_d) = 1000$ and $t_s/(L_d/v) = 0.001$. The contributions of gas- and surface-phase diffusions to the overall MSD are shown separately, with dashed and dotted lines, respectively.

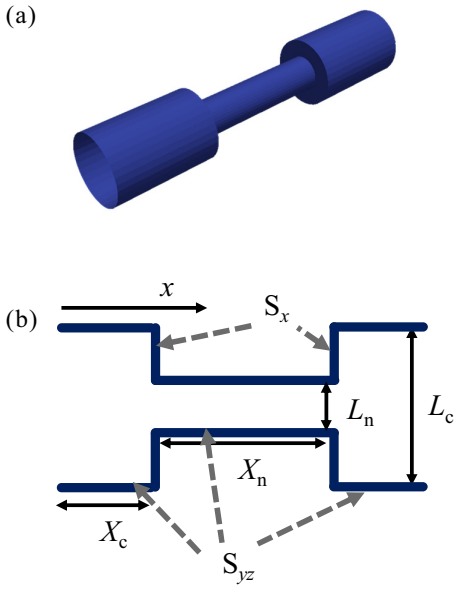

FIG. 6. Ink-bottle pore structure: (a) three-dimensional image, and (b) cross-sectional drawing.

C. Gas- and surface-phase diffusions in the ink-bottle pore

While the cylindrical pore utilized in Sec. III B has only a single diameter, actual porous media have a pore size distribution. To model the tortuosity of the structures, gas diffusion simulations are performed in the ink-bottle pores shown in Fig. 6. We denote the diameters of the cavity and neck by L_c and L_n, and their lengths by X_c and X_n, respectively. The ratio of the diameters, L_n/L_c, is set to 0.2 or 0.5. The lengths are set to $X_c = 1.25L_c$, $X_n = 2.5L_c$. We define L_c as the characteristic pore length. The diffusion coefficients in these structures are calculated by the MSD method. A periodic boundary condition is imposed on the x direction. t_s is fixed at $5.0 \times 10^{-6}\, L_c/v$, which is sufficiently small. The analytical solution given by Eq. (4) is only applicable to straight structures. It can be extended to tortuous structures as [29]

$$D = \frac{\varepsilon}{\tau_g} D_g + \frac{1}{\tau_s} \frac{D_s t_s}{t_g}, \tag{8}$$

where τ_g is the tortuosity factor and τ_s is the surface tortuosity factor. The trends of the calculation results are discussed on the basis of Eq. (8). The results are fitted to Eq. (8), by treating $D_s t_s$ as an independent variable and τ_s as a fitting parameter. $\varepsilon D_g/\tau_g$ is calculated by the MSD method with $D_s = 0$ and $t_s = 0$; it is then substituted into the first term on the right-hand side of Eq. (8). As for the t_g values, our simulations confirm that they are almost independent of D_s. For L_n/L_c ratios of 0.2 and 0.5, the $t_g/(L_c/v)$ values are 0.745 and 0.755, respectively. Figure 7 shows that the diffusion coefficients obtained by the simulations can be reasonably fitted to Eq. (8). For L_n/L_c ratios of 0.2 and 0.5, the τ_s values are 9.0 and 3.0, respectively. However, the curve fit for $L_n/L_c = 0.2$ shows a slight deviation compared with that for $L_n/L_c = 0.5$ in the region $(D_s t_s)^{0.5}/L_c < 1$.

In the above fitting, $\varepsilon D_g/\tau_g$ and τ_s are assumed to be uniquely determined by the given structures. To validate this assumption, diffusion phenomena in gas and surface phases have been analyzed by extracting individual MSDs of molecular motion in gas and surface phases, as demonstrated in Sec. III B. Since the diffusion coefficients calculated from the MSD on the surface are equal to the second term on the right-hand side of Eq. (8), τ_s can be obtained accordingly. Here we omit the modification factor ε in Eq. (2) since this factor is irrelevant to surface diffusion [29]. Figure 8 shows the calculated results for τ_s. It is found that τ_s increases with increasing $D_s t_s$. When $(D_s t_s)^{0.5}/L_c$ is less than 0.01, the τ_s values are slightly larger than unity: 1.2 and 1.1 for $L_n/L_c = 0.2$ and 0.5, respectively. This small difference can be explained by the directions of the surface normal vectors. As shown in Fig. 6, there are two kinds of surfaces: surfaces whose normal vectors are parallel to the x direction (S_x), and those whose normal vectors are orthogonal to the x direction (S_{yz}). Surface diffusion on S_x never contributes to the molecular transport in the x direction, resulting in a slightly larger τ_s. In fact, the calculated values of τ_s coincide with $(A_x + A_{yz})/A_{yz}$, where A_x is the area of S_x, and A_{yz} is the area of S_{yz}. By contrast, the increase in τ_s for $(D_s t_s)^{0.5}/L_c > 0.01$ in the case of $L_n/L_c = 0.2$ is due to another mechanism. A larger $D_s t_s$ leads to a longer surface diffusion distance, in which case molecules are more likely to go around the circumference of the neck entrance and be confined in the cavity. This significantly hinders the displacement in the x direction and thus the MSD decreases. We note that while the above fitting gives $\tau_s = 9.0$ and 3.0 for $L_n/L_c = 0.2$ and 0.5, respectively, the values calculated by the MSD of surface diffusion are 4.5 and 1.9, respectively, in the high $(D_s t_s)^{0.5}/L_c$ region. This discrepancy arises because

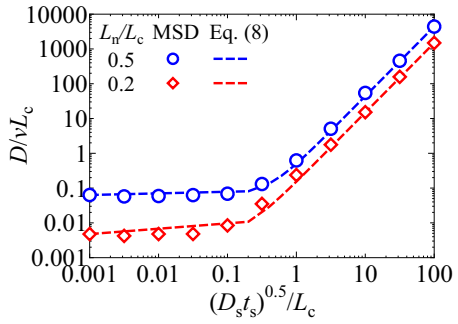

FIG. 7. Diffusion coefficients for ink-bottle pores, calculated by the MSD method. The results are fitted to Eq. (8). The Knudsen number is set to infinity.

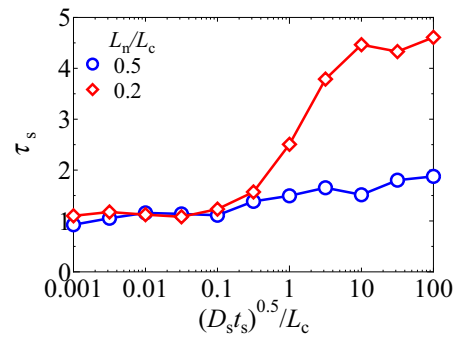

FIG. 8. Surface tortuosity factors of ink-bottle pores, calculated from surface-phase MSDs and Eq. (8).

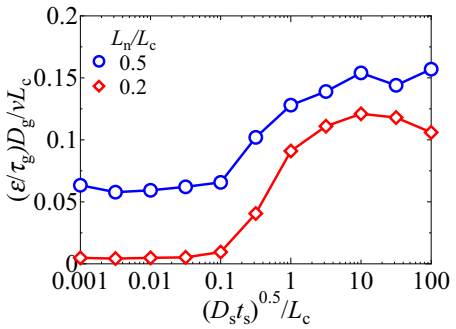

FIG. 9. Diffusion coefficient contributions from gas-phase diffusion in ink-bottle pores.

the porosity factor ε is not considered in the evaluation of τ_s. Indeed, given that $\varepsilon = 0.52$ and 0.625 for $L_n/L_c = 0.2$ and 0.5, the τ_s values can be said to agree well.

Next, the diffusion coefficients in the gas phase, D_g, are evaluated by utilizing the individual MSDs. Interestingly, D_g increases with $D_s t_s$, as shown in Fig. 9. There are two possible reasons for this. The first is that surface diffusion changes the correlation between the molecular velocities in the gas phase before and after collisions with the surface. More specifically, when molecules collide with S_x and immediately desorb from it, the collision always results in a reduction in molecular displacements in the x direction in the gas phase. However, this does not necessarily happen in the presence of surface diffusion; the correlation between the velocities in the x direction before absorption and after desorption is not always negative, owing to the displacement on the surface. The second possible reason for the increase in D_g with $D_s t_s$ is the change in the probability distribution of adsorption and desorption sites caused by surface diffusion. For example, if the probability of desorption from S_x is raised by surface diffusion, the expected velocity in the x direction in the gas phase increases. In order to investigate this second possibility, we measure the frequencies of adsorption and desorption at S_x and S_{yz}. We find that the probabilities of adsorption and desorption at S_x and S_{yz} for any $D_s t_s$ simply correspond to the ratio of the areas of these surfaces. This indicates that the second reason cannot explain the above-mentioned tendency. Thus the increase in diffusion coefficients in the gas phase can be attributed to the change in the correlation of the direction of motion in the gas phase due to surface diffusion.

As mentioned earlier in this section, it is found that gas- and surface-phase diffusions have a mutual influence on each other by utilizing the simulations where the molecules diffuse in two phases alternately by repeating adsorption and desorption on the surfaces. This effect has never been considered in Eq. (8), where the two transports are independent of each other and thus both $\varepsilon D_g/\tau_g$ and τ_s are constant for any $D_s t_s$. Nevertheless, a fit to Eq. (8) can reasonably represent the calculation results, as seen in Fig. 7. This is because the enhancement in surface diffusion counteracts the suppression of gas-phase diffusion, which coincidentally leads to a comparable overall diffusivity; as $D_s t_s$ increases, $1/\tau_s$ decreases while $\varepsilon D_g/\tau_g$ increases. Owing to this mutual influence, the type of simultaneous calculation presented in this study is necessary for an accurate evaluation of the diffusion coefficient in systems where both gas- and surface-phase diffusion occurs.

IV. CONCLUSIONS

Molecular transport simulations were performed to determine the effect of surface diffusion on the total diffusivity in simple cylindrical and ink-bottle pores. We incorporated the surface diffusion phenomenon into the two well-known simulation techniques: the test particle technique and mean square displacement technique. For a simple cylindrical pore, the diffusion coefficient in the presence of surface diffusion, as calculated by the test particle method, successfully reproduced the previously reported analytical solution. We also found that the diffusion coefficients evaluated by the two methods are related to each other through the ratio of gas- and surface-phase diffusion times. Finally, the diffusion coefficients of gas- and surface-phase diffusion were calculated separately for ink-bottle pores. The individual diffusion coefficients contributed by each mechanism clearly showed that gas-phase and surface-phase diffusions have a mutual influence on each other. In the presence of gas-phase diffusion, the surface diffusion is ended by desorption before the surface tortuosity effect becomes pronounced. Meanwhile, the gas-phase diffusion is enhanced by the surface diffusion, which makes it more likely for molecules confined in a cavity to enter the neck. Thus elucidating the diffusion phenomenon in meso- and micropores necessitates numerical calculations that simultaneously take account of molecular motions in both the gas and surface phases.

ACKNOWLEDGMENTS

This work was partly supported by New Energy and Industrial Technology Development Organization (NEDO) of Japan and JSPS KAKENHI Grant No. 16K18009.

[1] R. W. Baker, Ind. Eng. Chem. Res. **41**, 1393 (2002).
[2] P. Bernardo, E. Drioli, and G. Golemme, Ind. Eng. Chem. Res. **48**, 4638 (2009).
[3] J. R. Li, R. J. Kuppler, and H. C. Zhou, Chem. Soc. Rev. **38**, 1477 (2009).
[4] Y. Wang, J. Electrochem. Soc. **156**, B1134 (2009).
[5] W. Yuan, Y. Tang, X. J. Yang, and Z. P. Wan, Appl. Energy **94**, 309 (2012).
[6] J. J. Wang, L. Chen, Q. J. Kang, and S. S. Rahman, Int. J. Heat Mass Transfer **95**, 94 (2016).
[7] L. Wang, S. H. Wang, R. L. Zhang, C. Wang, Y. Xiong, X. S. Zheng, S. R. Li, K. Jin, and Z. H. Rui, J. Nat. Gas Sci. Eng. **37**, 560 (2017).
[8] G. A. Bird, *Molecular Gas Dynamics and the Direct Simulation of Gas Flows*, Oxford Engineering Science Series Vol. 42 (Clarendon Press/Oxford University Press, Oxford/New York, 1994).

[9] M. H. Abbasi, J. W. Evans, and I. S. Abramson, AlChE J. **29**, 617 (1983).
[10] A. Einstein, *Investigations on the Theory of the Brownian Movement* (Methuen & Co. Ltd., London, 1926).
[11] J. M. Zalc, S. C. Reyes, and E. Iglesia, Chem. Eng. Sci. **59**, 2947 (2004).
[12] S. Russ, Phys. Rev. E **80**, 061133 (2009).
[13] X. Michalet, Phys. Rev. E **82**, 041914 (2010).
[14] A. Berson, H.-W. Choi, and J. G. Pharoah, Phys. Rev. E **83**, 026310 (2011).
[15] M. Palombo, A. Gabrielli, V. D. Servedio, G. Ruocco, and S. Capuani, Sci. Rep. **3**, 2631 (2013).
[16] J. G. Choi, D. D. Do, and H. D. Do, Ind. Eng. Chem. Res. **40**, 4005 (2001).
[17] I. Medved and R. Cerny, Microporous Mesoporous Mater. **142**, 405 (2011).
[18] E. M. Reed and J. B. Butt, J. Phys. Chem. **75**, 133 (1971).
[19] Y. Shindo, T. Hakuta, H. Yoshitome, and H. Inoue, J. Chem. Eng. Jpn. **16**, 120 (1983).
[20] T. Okubo and H. Inoue, J. Chem. Eng. Jpn. **20**, 590 (1987).
[21] A. Tuchlenski, P. Uchytil, and A. Seidel-Morgenstern, J. Membr. Sci. **140**, 165 (1998).
[22] I. Prasetyo, H. D. Do, and D. D. Do, Chem. Eng. Sci. **57**, 133 (2002).
[23] G. W. Sears, J. Chem. Phys. **22**, 1252 (1954).
[24] F. G. Ho and W. Strieder, Chem. Eng. Sci. **36**, 253 (1981).
[25] J. R. Wolf and W. Strieder, J. Membr. Sci. **49**, 103 (1990).
[26] V. V. Levdansky, J. Smolik, and P. Moravec, Int. J. Heat Mass Transfer **51**, 2471 (2008).
[27] A. Pekalski and M. Ausloos, Surf. Sci. **344**, L1271 (1995).
[28] R. Holyst, D. Plewczynski, A. Aksimentiev, and K. Burdzy, Phys. Rev. E **60**, 302 (1999).
[29] J. M. Zalc, S. C. Reyes, and E. Iglesia, Chem. Eng. Sci. **58**, 4605 (2003).
[30] J. Zhang, J. Fan, and F. Fei, Phys. Fluids **22**, 122005 (2010).
[31] M. Knudsen, *The Kinetic Theory of Gases. Some Modern Aspects*, 3d ed., Methuen's Monographs on Physical Subjects (Methuen/Wiley, London/New York, 1950).
[32] D. Frenkel and B. Smit, *Understanding Molecular Simulation: From Algorithms to Applications* (Academic Press, San Diego, CA, 1996).
[33] A. Caravella, P. F. Zito, A. Brunetti, E. Drioli, and G. Barbieri, Microporous Mesoporous Mater. **235**, 87 (2016).
[34] N. Miyoshi, K. Osuka, I. Kinefuchi, S. Takagi, and Y. Matsumoto, J. Phys. Chem. A **118**, 4611 (2014).
[35] J. Rybka, A. Holtzel, S. M. Melnikov, A. Seidel-Morgenstern, and U. Tallarek, Fluid Phase Equilib. **407**, 177 (2016).
[36] R. D. Present, *Kinetic Theory of Gases*, International Series in Pure and Applied Physics (McGraw-Hill, New York, 1958).
[37] T. Hori, J. Shiomi, and C. Dames, Appl. Phys. Lett. **106**, 171901 (2015).